The Role of Proline and Glycine in Determining the Backbone Flexibility of a Channel-Forming Peptide

Jaison Jacob,* Herve Duclohier,# and David S. Cafiso*

*Department of Chemistry and Biophysics Program at the University of Virginia, Charlottesville, Virginia 22901 USA, and #UMR 6522 CNRS-University of Rouen (IFRMP 23), 76821 Mont Saint Aignan, France

ABSTRACT Alamethicin is a helical 20-amino acid voltage-gated channel-forming peptide, which is known to exhibit segmental flexibility in solution along its backbone near α-methylalanine (MeA)-10 and Gly-11. In an α-helical configuration, MeA at position 10 would normally hydrogen-bond with position 14, but the presence of proline at this position prevents the formation of this interhelical hydrogen bond. To determine whether the presence of proline at position 14 contributes to the flexibility of this helix, two analogs of alamethicin were synthesized, one with proline 14 replaced by alanine and another with both proline 14 and glycine 11 replaced by alanine. The C-termini of these peptides were derivatized with a proxyl nitroxide, and paramagnetic enhancements produced by the nitroxide on the Cα protons were used to estimate r^{-6} weighted distances between the nitroxide and the backbone protons. When compared to native alamethicin, the analog lacking proline 14 exhibited similar C-terminal to Cα proton distances, indicating that substitution of proline alone does not alter the flexibility of this helix; however, the subsequent removal of glycine 11 resulted in a significant increase in the averaged distances between the C- and N-termini. Thus, the G-X-X-P motif found in alamethicin appears to be largely responsible for mediating high-amplitude bending motions that have been observed in the central helical domain of alamethicin in methanol. To determine whether these substitutions alter the channel behavior of alamethicin, the macroscopic and single-channel currents produced by these analogs were compared. Although the substitution of the G-X-X-P motif produces channels with altered characteristics, this motif is not essential to achieve voltage-dependent gating or alamethicin-like behavior.

INTRODUCTION

In water-soluble proteins proline is a potent helix breaker; as a result, its relatively high frequency in the putative transmembrane (TM) helices of integral membrane proteins is somewhat surprising. Several structural and dynamic roles have been suggested for proline in transmembrane helices (Williams and Deber, 1991). It has been estimated that prolines bend helices by an angle of ~10–20 Å (Barlow and Thornton, 1988; Richardson and Richardson, 1989; Sankararamakrishnan and Vishveshwara, 1990), and proline-induced kinks are proposed to facilitate helical packing motifs (Woolfson and Williams, 1990). Because prolines are conserved in homologous transmembrane domains of channels, it has been suggested that they may provide ligand binding sites for cations (Sansom, 1992). Prolines have one fixed dihedral angle; for this reason, segments containing proline should have more rigidity and may provide a locus for protein folding and assembly (Li et al., 1996). The slow interconversion between the *cis/trans* peptidyl-prolyl bond is thought to be a rate-limiting step in the folding of some proteins (Fischer, 1995; Grathwohl and Wuthrich, 1981; Reimer et al., 1997), and in membrane proteins, this isomerization has been suggested as a mechanism to regulate the opening and closing of ion channels (Brandl and Deber, 1986; Helluin et al., 1998).

There are relatively few high-resolution structural data on membrane proteins and relatively few experimental data on the dynamics of transmembrane helices containing proline. In a series of model peptides rich in alanine and methylalanine, molecular dynamics calculations and fluorescence energy transfer were used to investigate the flexibility of peptides into which proline was inserted (Vogel et al., 1993). This work indicated that proline could act as a flexible element that mediated rigid body motions of helical segments. Circular dichroism has also been used to examine the effect of proline on the conformation of a number of model peptides in aqueous and nonaqueous environments (Li et al., 1996). This work suggests that while proline is a potent helix breaker in aqueous solution, it does not act as a helix breaker in hydrophobic environments. Proline does, however, act to disrupt β-sheet structures irrespective of the environment. Thus, the structural propensity of proline appears to be a function of the peptide or protein environment.

A number of membrane-active peptides that promote ion channel activity, such as melittin, cecropin, and alamethicin, contain proline residues (Bechinger, 1997). In addition, proline is frequently found with glycine in peptide channels as well as within the putative transmembrane domains of several membrane ion channels (Sessions et al., 1998). In alamethicin and melittin the motifs G-X-X-P and G-X-P are found, respectively, within the central portion of the helix. Alamethicin, a 20-amino acid voltage-gated peptide, contains proline at positions 2 and 14. The proline at position 2 may be important in stabilizing the helix end and providing an N-terminal cap for the peptide (Richardson and Richardson, 1988); in addition, this cap may be important in low-

Received for publication 6 July 1998 and in final form 8 December 1998.

Address reprint requests to Dr. David S. Cafiso, Department of Chemistry, University of Virginia, Charlottesville, VA 22901. Tel.: 804-924-3067; Fax: 804-924-3710; E-mail: cafiso@virginia.edu.

0006-3495/99/03/1367/10 $2.00

ering the energy for inserting the N-terminus of alamethicin into the membrane hydrocarbon (Barranger-Mathys and Cafiso, 1996). Alamethicin analogs that lack proline at position 14 also exhibit voltage-dependent gating; however, the lifetime and conductance states of the channel are altered. If proline is replaced at position 14 by alanine or if it is moved to different positions in the alamethicin sequence, higher conductance states are not as easily attained and the lifetimes of the conducting states are reduced (Duclohier et al., 1992; Kaduk et al., 1997).

Magnetic resonance studies on alamethicin in SDS micelles and in methanol indicate that alamethicin is a flexible helix in these environments. When simulated annealing is carried out on NMR-determined bond angle and distance constraints for alamethicin in SDS, both linear and bent forms of the peptide are obtained (Franklin et al., 1994). The linear and bent forms, which are shown in Fig. 1, exhibit conformational variability primarily in the ϕ and ψ angles of MeA-10 and Gly-11, but do not show conformational heterogeneity about Pro-14. One explanation for the conformational variability obtained from the simulated annealing, which also explains the reduction in NOEs detected in the central portion of the bilayer, is that the peptide is dynamic and converts between the two conformational forms shown in Fig. 1. To demonstrate that the peptide spends time in a bent configuration, a nitroxide spin-label was attached to the C-terminus of alamethicin, and paramagnetic enhancements of nuclear relaxation were obtained for alamethicin in methanol (North et al., 1994). In systems with large segmental motions, paramagnetic enhancements of nuclear relaxation nearly provide a distance of closest approach, because distances measured by this technique are weighted by r^{-6}. The distances obtained with this method are much shorter than those expected for a linear structure, indicating that the peptide spends at least a fraction of time in a highly bent configuration (Fig. 1). In the case of alamethicin, this work indicates that proline itself is not the residue about which N- and C-terminal helical segments are flexible; however, in an α-helical configuration, the carbonyl oxygen of MeA-10 would normally be hydrogen-bonded to position 14, an interaction that cannot occur with proline. Indeed, in its crystal structure, the carbonyl oxygen of MeA-10 is hydrogen-bonded to the solvent (Fox and Richards, 1982). As a result, one might expect the observed conformational variability about the ϕ and ψ angles of MeA-10 and Gly-11 to arise in part from the presence of proline at position 14. Recent dynamics simulations in methanol are consistent with the findings from NMR and indicate that alamethicin can undergo large structural fluctuations in the central portion of the helix (Gibbs et al., 1997; Sessions et al., 1998). These fluctuations involve flips of peptide bonds involving Gly-11, a process that could be a result of the loss of hydrogen-bonding constraints on Aib-10 as well as the absence of β-atoms on Gly-11.

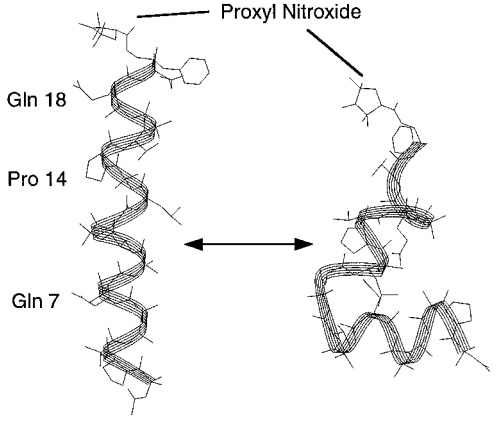

FIGURE 1 Bent (*left*) and linear (*right*) forms of alamethicin having a proxyl-nitroxide derivatized to the peptide C-terminus. The bent form is obtained from an NMR structure previously determined in SDS micelles (Franklin et al., 1994), while the linear form is obtained from the peptide crystal structure (Fox and Richards, 1982). In each case a spin-label has been appended to the C-terminus and the structure energy minimized. Previous work has shown that distances obtained by long-range paramagnetic enhancements of nuclear relaxation are consistent with the interconversion of these two forms in methanol (North et al., 1994).

In the present work we investigated the contributions that Pro-14 and Gly-11 make to the observed conformational flexibility of alamethicin in solution. We synthesized two analogs of alamethicin, which are shown in Table 1, where nitroxide spin-labels are derivatized to the C-terminus of the peptide. Paramagnetic enhancements of ^{1}H nuclear magnetic spin-lattice relaxation produced by the spin-label were then used to probe the role of proline 14 and glycine 11 in determining the flexibility of alamethicin. The NMR results demonstrate that while proline 14 alone has little effect on the ability of alamethicin to bend in solution, the substitution of both glycine 11 and proline 14 to alanine dramatically affects the average peptide conformation. Macroscopic and single-channel current recordings of these analogs indicate that while the loss of the G-X-X-P motif in alamethicin produces channels with somewhat altered characteristics, it is not essential to achieve voltage dependence in this channel.

EXPERIMENTAL PROCEDURES

Materials

Fmoc-protected amino acids were purchased from Calbiochem-Novabiochem Corp., and alkoxybenzyl alcohol resins were purchased from BaChem Bioscience Inc. (Bubendorf, Switzerland). Cyanuric fluoride was obtained from Pfaltz and Bauer (Waterbury, CT), and 3-aminomethyl-PROXYL and alamethicin were purchased from Sigma (St. Louis, MO). CD_3OD and CD_3OH were obtained from Cambridge Isotopes Limited (Woburn, MA). Palmitoyloleoylphosphaditylcholine (POPC) and dioleoylphosphatidylethanolamine (DOPE) were purchased from Avanti Polar Lipids (Alabaster, AL).

Synthesis and labeling of peptides

Native alamethicin with a proxyl nitroxide attached to its C-terminus was synthesized as previously described (Archer et al., 1991). Two peptides, one in which Pro-14 was replaced by Ala (P14A) and another in which

TABLE 1 Sequence of alamethicin and alamethicin analogs

Peptide	Sequence*
Alamethicin	Ac-MeA-Pro-MeA-Ala-MeA-Ala-Gln-MeA-Val-MeA-Gly-Leu-MeA-**Pro**-Val-MeA-MeA-Gln-Gln-Phol
P14A	Ac-MeA-Pro-MeA-Ala-MeA-Ala-Gln-MeA-Val-MeA-Gly-Leu-MeA-**Ala**-Val-MeA-MeA-Gln-Gln-Phe
PGA	Ac-MeA-Pro-MeA-Ala-MeA-Ala-Gln-MeA-Val-MeA-**Ala**-Leu-MeA-**Ala**-Val-MeA-MeA-Gln-Gln-Phe

*MeA is α-methylalanine. The sequence of alamethicin isolated and studied here is one of four metabolites present in alamethicin that is available from Sigma (St. Louis, MO) (Kelsh et al., 1992). Amino acids in bold indicate proline 14 and alanine substitutions.

both Pro-14 and Gly-11 (PGA) were replaced by Ala, were synthesized on a model 433A Applied Biosystems Inc. peptide synthesizer. The Fmoc-protected amino acids were converted to Fmoc-protected aminoacyl fluorides as described previously (Wenschuh et al., 1995), and a general deprotection scheme was employed (Stewart and Young, 1984). Residue coupling involved agitation of the Fmoc-deprotected resin for 45 min in the presence of a fivefold excess of both the aminoacyl fluoride and diisopropylethylamine (DIEA). N-terminal acetylation was carried out by treating the peptide with a 20% solution of acetic anhydride and 10% DIEA in dimethylformamide (DMF) for 30 min before cleavage. The peptides were cleaved with 95% trifluoroacetic acid (TFA) and 5% triethylsilane. To spin-label the peptides, the crude peptides were reacted with five equivalents of 3-aminomethyl-PROXYL, half equivalent of dimethylaminopyridine, one equivalent of DIEA, and three equivalents of 2-(^{1}H-benzotriazole-1-yl)-1,1,3,3-tetramethyluronium hexafluorophosphate (HBTU) in 4:1 acetonitrile:DMF for several hours. At the end of the reaction period the mixture was lyophilized. For purification, a methanolic solution was applied to a semipreparative Vydac reverse phase C18 HPLC column and eluted using a flow rate of 3 ml/min and a solvent system running between 70% A/30% B to 100% B in 35 min, where A was 0.05% aqueous TFA and B was acetonitrile with 0.05% TFA. The pure peptides eluted at ~28 min. The spin-labeled peptides were identified by EPR spectroscopy and the mass of all the peptides were confirmed by mass spectrometry.

NMR measurements

NMR spectra were obtained using either a GE Omega 500 or a Varian UnityPlus 500 NMR spectrometer. Proton chemical shift assignments were made from a solution containing 5 mM peptide in CD_3OH. Proton relaxation data were obtained from peptide samples dissolved in CD_3OD using a standard inversion recovery sequence, 180-τ-90-acquisition, with presaturation of the solvent peak. A typical measurement consisted of 13 data sets collected for τ values between 10 μs and 7 s. A 7-s relaxation delay was used between scans. For each data set, 64, 128, or 256 scans of 16K points were collected over a 5000 Hz sweep width. The spectra were processed using the Felix95 software (MSI, Scranton, CA), and the time domain data were multiplied with a 60° phase-shifted sine squared bell and Fourier-transformed. Baselines were corrected using the built-in automatic baseline flat routine, and the peak intensities were fitted with a three-parameter exponential function using MATLAB. The spectra and relaxation data for unlabeled P14A were taken at a concentration of ~3 mM, while the spectra and relaxation rates of spin-labeled P14A-SL were taken at seven concentrations from 1.8 mM to 0.8 mM. The spectra and relaxation rates for unlabeled PGA were taken at three concentrations between 3 mM and 0.5 mM and spin-labeled PGA-SL were investigated at nine concentrations between 1.9 mM and 0.4 mM. The values used in the distance calculations were the average of 2 (labeled) or 3 (unlabeled) separate measurements.

Estimating ^{1}H-nitroxide distances

The paramagnetic enhancement factor of the nuclear spin-lattice relaxation rate, R_1^{enh}, was calculated from the following equation:

$$R_1^{enh} = R_1^{para} - R_1^{diam} \quad (1)$$

where R_1^{diam} is the relaxation rate for the unlabeled peptide and R_1^{para} is relaxation rate of the labeled peptide at infinite dilution obtained by extrapolation to zero concentration. The distance between the nitroxide and the observed proton, r (in angstroms), was estimated using a simplified form of the Solomon-Bloembergen equation,

$$r = C\left\{\left(\frac{3\tau_C}{1+\omega_I^2\tau_C^2} + \frac{7\tau_C}{1+\omega_S^2\tau_C^2}\right)R_1^{enh}\right\}^{1/6} \quad (2)$$

where C is a constant having a value of 540 Å for protons, and ω_I and ω_S are the nuclear and electron Larmor frequencies (Krugh, 1976). This expression is generally valid for spin-labels where the electron relaxation times are long relative to the correlation time, τ_C. A value of 0.7 ns is used for τ_C, which corresponds to the effective overall correlation time for alamethicin rotation in methanol (Esposito et al., 1987). This choice of τ_c presumes that high-frequency motions in the picosecond time scale are of limited amplitude, an assumption that appears reasonable for these peptides. However, because the estimated distance depends upon the sixth root of the correlation time, the distances obtained from Eq. 2 are remarkably insensitive to the value of τ_C.

EPR spectroscopy

EPR spectra were obtained using a Varian E-line spectrometer and a standard X-band cavity resonator at a modulation amplitude of 1 G and a microwave power of 10 mW. The samples were placed in quartz capillaries of 10 μl volume at a concentration of ~100 μM. Estimates of the rotational correlation time for the nitroxide probe derivatized to the peptides shown in Table 1 were determined as described previously (Archer et al., 1991; Keith et al., 1970; Nordio, 1976). These estimates of rotational correlation time assume that the motion of the spin label is isotropic.

Planar bilayer measurements

The macroscopic conductances and single-channel activity induced by the PGA analog were assayed in planar lipid bilayers as previously described (Duclohier et al., 1992). Briefly, macroscopic conductances resulting from the activity of hundreds or thousands of channels were recorded in virtually solvent-free bilayers (Montal and Mueller, 1972) doped with peptide and exposed to slow voltage ramps (typically 1 min per cycle over a ±150 mV range). The bilayer was made by folding two lipid monolayers over a 150–200 μm hole in a PTFE film sandwiched between two half glass cells. The hole had been previously pretreated with a few microliters of a 4% hexadecane solution in hexane. The electrolyte on both sides of the bilayer was 1 M KCl, 10 mM Hepes (pH = 7.4). Voltage was delivered via an Ag/AgCl electrode on the *cis* side of the bilayer, (the *cis* side refers to the side of peptide addition and the electrically positive side of the bilayer). Currents are measured via a second electrode in the *trans* side connected to an amplifier and current-voltage converter.

For recordings of single-channel activity, bilayers were made at the tip of patch pipettes as described previously (Coronado and Latorre, 1983; Hanke et al., 1984), and a standard patch-clamp apparatus was used. Here, the peptide was added in the external bath but voltage was delivered and currents measured via an electrode on the inside of the pipette. Current recordings were analyzed with the Satori software (Intacell, Royston, UK).

In all cases, the lipids used to form bilayers were made from a mixture of neutral lipids consisting of POPC:DOPE (7:3).

RESULTS

The TOCSY spectra of both unlabeled and spin-labeled PGA are shown in Fig. 2. Resonances for the unlabeled PGA were assigned using standard 2-dimensional (2-D) experiments following the general protocol described elsewhere, except that a 2-D ROESY instead of a NOESY was used to determine the connectivities (Wuthrich, 1986). The two spectra in Fig. 2 are identical except for a few sets of crosspeaks that are absent in the spectra of the spin-labeled analog. Crosspeaks due to residue 15 and those closer to the C-terminus did not appear in the TOCSY spectra of the spin-labeled analog as a result of strong paramagnetic enhancements of nuclear relaxation. The absence of crosspeaks from residues closer to the spin label served as an independent check to confirm sequence specific assignments obtained from the ROESY spectra. For example, of the three Gln residues in the primary structure of the peptide, Gln-18 and Gln-19 are very close to the spin label and should not give rise to crosspeaks in the spectra of the spin-labeled analog. Therefore, the only the set of crosspeaks that arises from Gln should be due to Gln at position 7. This assignment is the same as that obtained using the ROSEY connectivities. In a similar manner, the TOCSY spectra also provided an easy assignment of Val-9 and Val-15, by inspection of the TOCSY spectra of the unlabeled and spin-labeled analogs.

Alanine-for-proline substitution does not alter Cα proton-nitroxide distances

Relaxation enhancements due to nitroxides in solution can be both intramolecular or intermolecular in origin. While the intermolecular contribution is strictly governed by translational diffusion of the molecules, it does not have any recoverable information on the internal dynamics of the peptide. However, the intramolecular contribution to relaxation enhancements is dictated by the dynamics of the molecule. The intramolecular contribution was determined by examining the concentration dependence of the paramagnetic enhancement of the relaxation rate. Shown in Fig. 3 (*A*) is plot of the paramagnetic contribution to the relaxation rate, R_1^{SL}, as a function of P14A-SL concentration for the Cα protons associated with Ala-4, Gln-7, and Ala-14. The intramolecular contributions, R_1^{para}, were obtained by extrapolating the linear concentration dependence of R_1^{SL} to infinite dilution and the values are summarized in Table 1. The relaxation enhancement factors due to the spin label, R_1^{enh}, were calculated from Eq. 1 and the corresponding nitroxide-proton distances were estimated using Eq. 2 and are summarized in Table 2. The nitroxide-proton distances calculated for P14A are not significantly different from that obtained for native spin-labeled alamethicin; in particular, the long-range distances measured for residues 2, 4, and 6 in P14A are very similar to those measured for alamethicin. A decrease in the flexibility of alamethicin about the central portion of the helix should have resulted in increased long-range distances, and these data indicate that substitution of Pro-14 with Ala does not change the flexibility exhibited by alamethicin in solution (see Fig. 4)

Substitution of both proline and glycine lengthens Cα proton-nitroxide distances

Fig. 3 *B* shows a plot of the relaxation rates as a function of concentration of the spin-labeled PGA-SL. The relaxation data and the calculated nitroxide-proton distances for PGA are summarized in Table 3. In general, PGA shows the same

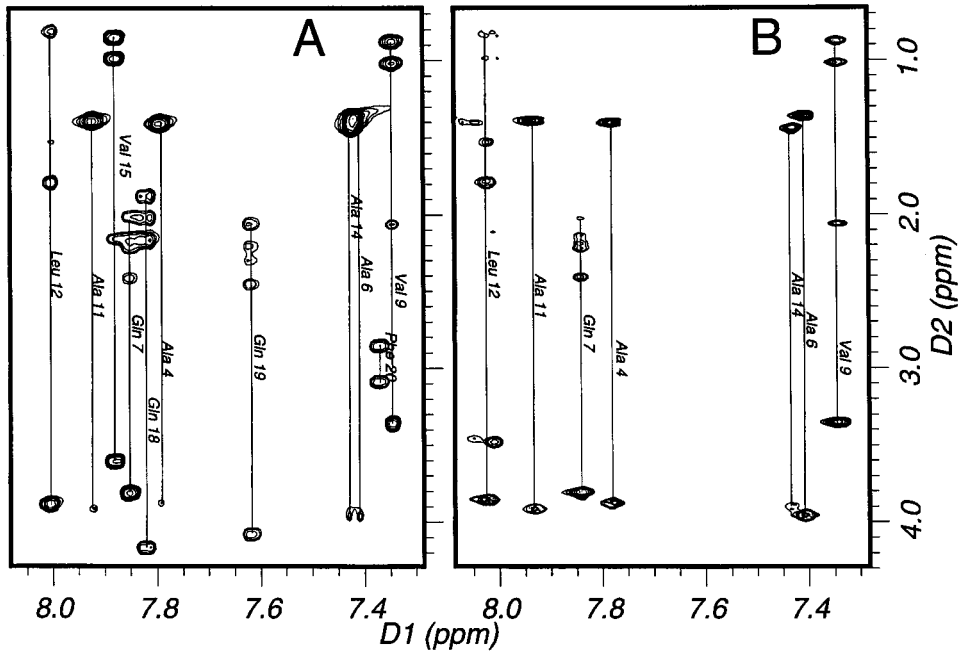

FIGURE 2 TOCSY spectra of PGA (*A*) and PGA-SL (*B*) showing the correlation of amide protons with the other protons in the spin-system. The chemical shifts are not altered by the presence of spin-label; however, crosspeaks from residues 15 and upward are not observed due to their spatial proximity to the nitroxide.

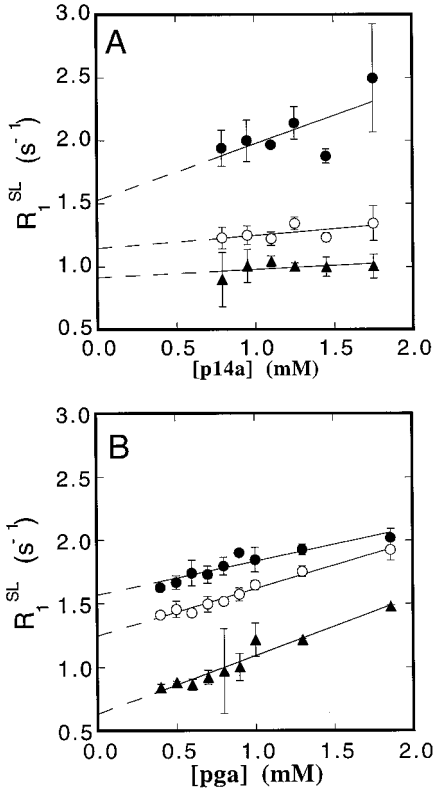

FIGURE 3 Plots of R_1^{SL} for the Ala-4 (●), Gln-7 (○), and Ala-14 (▲) Cα protons as a function of peptide concentration. The extrapolation of the data to infinite dilution gives the intramolecular rate, R_1^{para}, which is used to calculate the nitroxide-proton distances. The data for other positions show a similar behavior and the extrapolations to infinite dilution are shown in Tables 2 and 3.

trend as alamethicin and P14A: residues closer to the nitroxide spin-label have a faster relaxation rate than residues that are farther from it. However, for PGA, the nitroxide-Cα proton distances are longer at every distance than those measured for either alamethicin or P14A. In particular, residues 2, 4, 6, and 7 show distances that are considerably larger than those for alamethicin, and the simplest interpretation of these data is that the analog PGA (Table 1) is less flexible than alamethicin. It should be noted that the relaxation rate of Ala-4 in the spin-labeled and the unlabeled PGA are the same within experimental error. Given the experimental uncertainty in the measurements of R_1^{para}, we estimate that the averaged distance between the nitroxide and the Cα proton on Ala-4 must be at least 26 Å or greater.

Shown in Fig. 4 are the effective distances calculated using Eq. 2 for the three alamethicin analogs plotted as a function of residue position. In addition, Fig. 4 shows the expected distances for the energy-minimized crystal structure of alamethicin with a proxyl moiety attached to the C-terminus. The distances obtained by measuring NMR relaxation enhancements are much shorter than the distances in the crystal structure, and the nitroxide-proton distances obtained for P14A and alamethicin are approximately the same within experimental error. In general, differences in the distances obtained from NMR relaxation and from the crystal structure are largest at the N-terminal end of the peptide, where the differences for alamethicin and P14A are as much as 15 Å. The shorter measured distances seen for the spin-labeled analogs compared to the crystal structure may in part be due to flexibility about bonds linking the spin-label to the C-terminus. However, we estimate that rotation of bonds attaching the nitroxide to the peptide alone can only account for a shortening of the distances in the crystal structure by at most a few angstroms.

Motion of the C-terminal spin-label on alamethicin and alamethicin analogs

To determine whether there were differences in the motion of the spin-label on the nanosecond time scale, which might reflect significant differences in the motion of the C-terminus, EPR spectra of the three peptides in methanol were taken and are compared in Fig. 5. The EPR spectra of these peptides indicate that the label on each peptide undergoes similar rates of motion that are fast and slightly anisotropic. The rates of motion for the label can be estimated assuming an isotropic model, and effective correlation times of 0.16 ns, 0.28 ns, and 0.29 ns are found for the label on alamethicin-SL, P14A-SL, and PGA-SL, respectively. The C-terminal residue of native alamethicin is a reduced phenylalanine, and in this case the spin-label was attached through an ester linkage. The analogs P14A-SL and PGA-SL were synthesized with phenylalanine at their C-termini, and for these peptides the spin-label was attached through an amide linkage. The shorter correlation time observed for the label attached to native alamethicin is likely a result of the presence of this ester linkage. The two analogs where the label is attached through an amide linkage show slower but virtually identical rates of motion. In the present case, motion of the spin-label at the C-terminus appears to be insensitive to differences in the helix bending motion that occur between P14A-SL and PGA-SL.

The correlation time that is estimated for the spin-label should not be confused with the 0.9-ns correlation time that is used to estimate the overall rotational motion of the peptide. This longer correlation time describes the motion of the interspin N-O/Cα-H vector, and local motion about the spin-label and the observed Cα proton will further modulate this interaction. It is important to note that although the effective correlation time for each peptide and residue may be slightly different, the distances that are estimated are relatively insensitive to the choice of correlation time. As indicated above this occurs because distances estimated from the paramagnetic enhancement depend upon the sixth root of the correlation time (see Eq. 2).

Macroscopic and single-channel currents for PGA

The macroscopic and single-channel conductance properties of the alamethicin analog PGA were measured in planar

TABLE 2 Relaxation rates and standard errors in s^{-1} and nitroxide-Cα proton distances in angstroms for P14A and P14A-SL

Cα proton position	R_1^{para}	R_1^{diam}	R_1^{enh}	d
Pro-2	0.984 ± 0.010	0.804 ± 0.039	0.180	19.2
Ala-4	0.850 ± 0.040	0.773 ± 0.020	0.077	22.1
Ala-6	1.096 ± 0.020	0.791 ± 0.020	0.305	17.6
Gln-7	1.200 ± 0.040	0.894 ± 0.021	0.306	17.5
Val-9	1.347 ± 0.060	0.869 ± 0.061	0.478	16.3
Gly-11a	2.312 ± 0.043	1.504 ± 0.009	0.808	14.9
Gly-11b	2.238 ± 0.055	1.514 ± 0.044	0.724	15.2
Leu-12	1.731 ± 0.174	0.769 ± 0.009	0.962	14.5
Ala-14	2.104 ± 0.360	0.733 ± 0.006	1.371	13.7

R_1^{diam} is the relaxation rate of the unlabeled peptide and R_1^{para} is the relaxation rate for the spin-labeled peptide at infinite dilution obtained by linear extrapolation of R_1^{SL} as shown in Fig. 3. R_1^{enh} is the enhancement due to the spin label calculated using Eq. 1.

bilayers as described above. In POPC:DOPE bilayers, where the PGA analog is added to the *cis* side, the membrane exhibited macroscopic currents in response to slow voltage ramps that were typical of that seen for native alamethicin; that is, there was a steep exponential branch whose threshold was dependent on peptide concentration (see Fig. 6). Equilibration of the bilayer response to peptide addition required ~10 min as judged by the superposition of 3 to 5 current voltage traces, and this equilibration was about twice as fast as that for native alamethicin. Using an analysis applied previously for alamethicin (Hall et al., 1984), Va (the voltage threshold change produced by an e-fold change in peptide concentration) and Ve (the voltage increment required to produce an e-fold change in conductance) were determined from an average of three experiments. These data were also used to obtain an estimate for n, the apparent number of monomers that participate in the conducting aggregate. These data are summarized in Table 4 and indicate that the PGA analog is similar to alamethicin in the macroscopic currents it produces in bilayers.

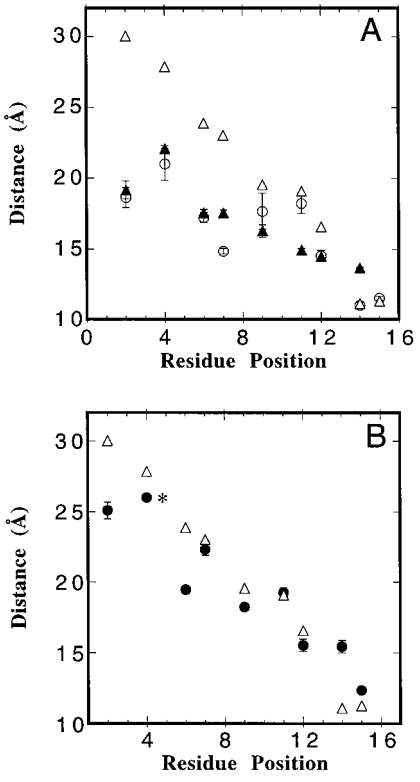

FIGURE 4 Nitroxide to Cα proton distances determined from the paramagnetic enhancements, R_1^{enh}. In (*A*) are shown distances for alamethicin (○), P14A (▲), and the expected distances from the crystal structure (△) of alamethicin. Distances for alamethicin and the crystal structure were taken from North et al., 1994, and were obtained from structure A in the subunit cell. The other two structures in the subunit cell are also linear and yield very similar distances. In (*B*) are shown distances for PGA (●) compared with those expected for the crystal structure (△) of alamethicin. *Due to the absence of any significant relaxation enhancement for this proton, we estimate the nitroxide-to-Cα proton distance for Ala-4 to be at least 26 Å or larger.

Fig. 7 shows single-channel events for the PGA analog in bilayers formed at the tips of patch pipettes. These events have a relatively large amplitude, but compared to native alamethicin, they have a rather low probability of opening and a short duration. This behavior and the activity shown in Fig. 7 *A* are similar to that obtained for the P14A analog (Kaduk et al., 1997). Compared with native alamethicin both of these analogs have fewer open substates, and transitions among higher conductance states, which are typical of alamethicin, are rarely encountered. The voltage-dependence of the probabilities for single-channel conductance states was found to be in approximate agreement with the value of Ve determined from macroscopic conductance measurements. Table 4 summarizes the data from both the macroscopic and single-channel conductance measurements for alamethicin, P14A, and PGA. The most significant differences between the P14A and PGA analog are a significantly lower value of Va for P14A, and a much lower conductance for the first conducting state of PGA.

DISCUSSION

Paramagnetic enhancements of nuclear relaxation were used here to investigate the amplitude of the helix-bending motion in several alamethicin analogs. This technique appears to be ideally suited to examine these high-amplitude motions. This measurement provides nearly a distance of closest approach between the nitroxide and observed proton, and in a peptide such as alamethicin the bending of the helix will result in much shorter distances than expected based

TABLE 3 Relaxation rates and standard errors in s^{-1} and nitroxide-Cα proton distances in angstroms for PGA and PGA-SL

Cα Proton Position	R_1^{para}	R_1^{diam}	R_1^{enh}	d
Pro-2	0.826 ± 0.065	0.790 ± 0.017	0.036	25.1
Ala-4	0.711 ± 0.090	0.740 ± 0.050	−0.030	
Ala-6	1.002 ± 0.103	0.838 ± 0.048	0.164	19.5
Gln-7	1.254 ± 0.146	1.182 ± 0.013	0.072	22.3
Val-9	1.225 ± 0.073	0.985 ± 0.038	0.241	18.3
Ala-11	1.029 ± 0.022	0.854 ± 0.019	0.175	19.3
Leu-12	1.544 ± 0.050	0.911 ± 0.016	0.633	15.5
Ala-14	1.433 ± 0.120	0.779 ± 0.008	0.654	15.5
Val-15	3.260 ± 0.200	0.784 ± 0.012	2.476	12.4

See legend to Table 2.

upon the rigid linear structure (North et al., 1994). The data obtained here show that there are dramatic differences between nitroxide-Cα proton distances expected from the crystal structure and those found in peptides such as alamethicin and P14A in solution (see Fig. 4). As discussed previously, spin diffusion is unlikely to explain such dramatic differences, as the electron-nuclear dipolar coupling is 4.3×10^5 times larger than that of a proton-proton coupling for a given interspin separation (North et al., 1994). The observed differences in the distances are most easily explained by a rapid averaging of the time-dependent intermoment distances governed by the internal motions of the peptide. An inspection of Fig. 4 shows that at shorter values of the intermoment separation, the differences between distances from the crystal structure and those from paramagnetic enhancements are small. This is reasonable, because low-amplitude motions have little effect on average intermoment distances, whereas high-amplitude segmental motions produce a more efficient averaging weighted toward the distance of closest approach.

The data shown above indicate that the N-O/Cα proton distances estimated for the P14A analog are very similar to those found for alamethicin. The fact that replacement of Pro-14 with a helix-favoring residue like Ala does not alter the distance of closest approach suggests that Pro-14 has very little influence on the high-amplitude motions exhibited by alamethicin in solution. This is not entirely surprising due to the rather restricted nature of one of the dihedral angles of proline caused by the cyclization of its side chain back to the backbone amide. The results reported here are consistent with a recent study indicating that in membrane mimetic environments and organic solvents, the helical propensity of proline is greatly enhanced. In these environments, proline appears to impart an additional thermal stabilization to α-helices (Li et al., 1996). In contrast, previous fluorescence work on MeA-containing peptides indicated that proline could act as a flexible hinge (Vogel et al., 1993). These earlier findings are not supported by the studies carried out here and previous work showing that alamethicin has little flexibility about Pro-14 (Franklin et al., 1994). The reasons for the differences between the NMR results

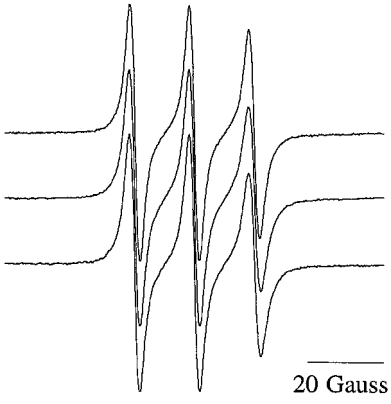

FIGURE 5 EPR spectra of spin-labeled analogs of alamethicin, P14A, and PGA in methanol (*top* to *bottom*). The EPR spectra for the PGA and P14A analogs are virtually identical and undergo identical rates of motion. The C-terminal spin-label attached to alamethicin undergoes slightly faster rates of motion, which is likely a result of the ester linkage connecting the proxyl nitroxide to the C-terminal phenylalaninol on native alamethicin.

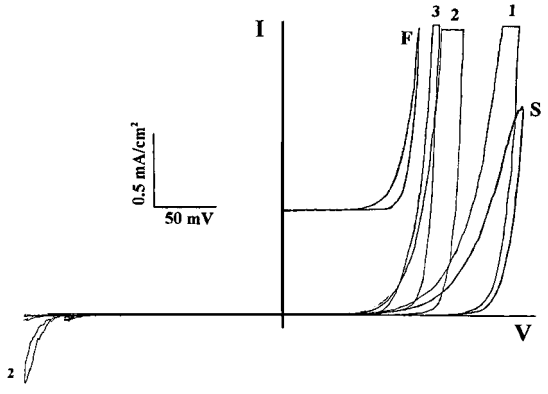

FIGURE 6 Macroscopic current-voltage (*I-V*) curves produced in planar bilayers by the addition of the PGA alamethicin analog at room temperature. The addition of 5×10^{-8} M PGA to the *cis* side of the bilayer from a methanolic stock solution results in the bold trace labeled S (*far right*) after equilibrium has been reached (this curve is the result of three sweeps recorded in response to slow voltage ramps). Further addition of PGA to a concentration of 1.5×10^{-7} M shifts the *I-V* curve to the left, and curves 1, 2, and 3 are obtained 1, 2, and 3 min after the addition. Note the asymmetric response between the positive and negative voltage axis. The small response in the negative quadrant was obtained 2 min after the second addition of peptide, after which the magnitude of the voltage ramp was reduced. Eight to 10 min after the second addition, a new steady-state *I-V* curve is reached, indicated by the curve F (this curve is displaced on the current axis for clarity).

TABLE 4 Conductance data from macroscopic and single channel recordings

Peptide	Va	Ve	⟨N⟩	γ (pS)
PGA	70	8	8 ± 1	80, 400, 1100, 2500
P14A	38	6	6 ± 1	170, 380, 1200, 2500
Alamethicin	60	6	10 ± 1	170, 400, 1300, 2500, 4000, 5600

The parameters Va, Ve, and ⟨N⟩ are determined as previously described (Hall et al., 1984). The data for alamethicin and P14A were taken from Kaduk et al., 1997.

and the fluorescence work are not clear. The two studies were carried out in the same solvent system, but the peptides used in these two experiments are not identical.

The distance estimates obtained for the PGA analog indicate that the replacement of both proline and glycine in the central domain of alamethicin dramatically reduces the high-amplitude hinge motion of this helix. When the G-X-X-P motif in alamethicin is replaced by A-X-X-A, the distance of closest approach between the N-terminal residues and the C-terminal nitroxide is altered by as much as 6 Å. The simplest interpretation of this result is that these substitutions alter the dynamics of the peptide backbone, and that the PGA analog is more rigid than either alamethicin or the P14A analog. Although we did not test the effect of replacing Gly-11 alone, its role is likely to be significant. For a peptide in solution, replacement of glycine by alanine should reduce the conformational entropy of the peptide backbone (D'Aquino et al., 1996), and the importance of Gly-11 in alamethicin is indicated by dynamics simulations, which show that the peptide flexibility in methanol can be attributed to H-bond flips involving this residue (Gibbs et al., 1997; Sessions et al., 1998).

Macroscopic and single-channel conductances were measured for the PGA analog to determine the effect of removing the G-X-X-P motif on the channel activity. Previous work indicated that substituting Pro-14 limits the capacity of the peptide to achieve stable high-level conductance states and lyse cells (Dathe et al., 1998; Kaduk et al., 1997). The channel recordings obtained here demonstrate that the PGA analog retains a high voltage-dependence and the apparent number of monomers participating in the conductive aggregate is similar to that of alamethicin. Like the P14A analog, the PGA analog shows fewer open substates and the channel kinetics of the PGA analog are faster than that of alamethicin. The difference in the value of Va for the P14A analog when compared to either alamethicin or PGA may be a result of the reduced hydrophobicity of the P14A analog, and indeed EPR measurements on this analog indicate that it has a weaker membrane binding relative to native alamethicin (Lewis and Cafiso, unpublished results). The reduced conductance for the first open level of the PGA analog suggests that the smallest conducting aggregate for this peptide has a smaller pore than P14A or native alamethicin. This could be due to differences in the dynamics

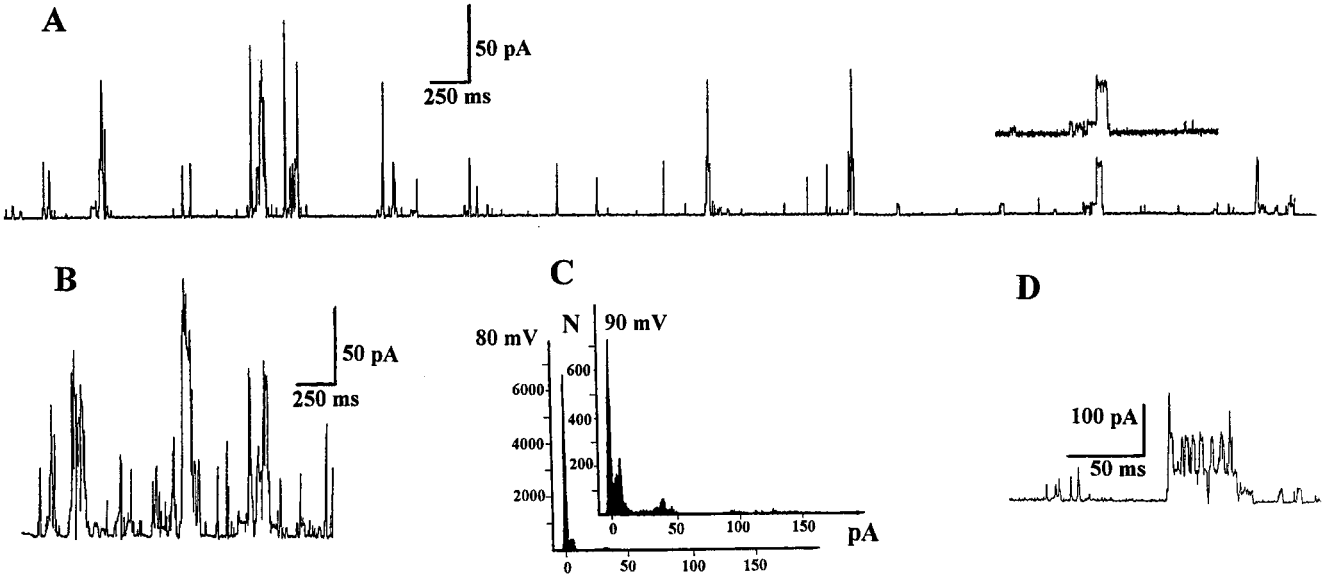

FIGURE 7 Single-channel currents induced by the alamethicin analog PGA at a concentration of 5×10^{-8} M and obtained at a temperature of 12°C. (*A*) A 10-s recording using a 300 Hz filter at an applied voltage of 80 mV, indicating a low probability of channel opening with evidence for transitions between subconductance states (evidence for these transitions is clearly seen in the *inset* where the time base is divided by 2 and a 1 kHz filter is used). (*B*) A short recording of the bilayer in (*A*) at an applied potential of 90 mV. (*C*) Two conductance histograms showing the number of channel events as a function of conductance at two voltages. (*D*) A short stretch of fast channel activity obtained at 18–20°C. The fluctuation between substates is similar to that seen for alamethicin, but occurs with much faster kinetics.

of the backbone, which may not allow structural fluctuations necessary for the passage of ions in the smallest aggregate, but it may also be a result of the substitution of a methyl group for a proton within the central portion of the channel.

It should be emphasized that the high-amplitude helix-bending motion seen here in methanol does not appear to occur in bilayers (at least in the absence of voltage). For example, measurements in bilayers using ^{15}N-NMR and EPR spectroscopy indicate that alamethicin is in a linear configuration along the bilayer normal, and it does not appear to be present in a bent configuration within the membrane (Barranger-Mathys and Cafiso, 1996; North et al., 1994). This is not entirely unexpected, as the membrane environment provides little opportunity for the rapid interconversion of intramolecular hydrogen bonds. Thus, we do not expect these analogs to have conformations that are as different from each other in the membrane as they are in solution.

In conclusion, the results presented here demonstrate that the high-amplitude bending motion that is observed for alamethicin in solution can be attributed to the G-X-X-P motif in the central portion of the peptide. In the present case, proline does not act as a flexible hinge between the two helical regions that flank it, and introducing the potential for hydrogen bonding between position 14 and MeA-10 alone does not alter the peptide flexibility. The removal of the G-X-X-P does not produce a channel that is significantly different from alamethicin, except that it does not as easily achieve highly conductive substates. Finally, the work described here demonstrates that paramagnetic enhancement of nuclear relaxation can be a valuable tool to investigate large amplitude motions in peptides and other macromolecules. Paramagnetic enhancements of nuclear relaxation were first suggested more than 30 years ago as a method to determine distances in proteins (McConnell, 1967; Sternlicht and Wheeler, 1967), but they have not been widely utilized for structure determination. In molecules such as alamethicin that have large segmental motions, paramagnetic enhancements provide long-range $\langle r^{-3}\rangle^2$ weighted distances that can provide an upper bound on the distance of closest approach between an electron and nucleus.

This research was supported by National Institutes of Health Grant GM-35215 (to D.S.C.).

REFERENCES

Archer, S. J., J. F. Ellena, and D. S. Cafiso. 1991. Dynamics and aggregation of the peptide ion channel alamethicin. *Biophys. J.* 60:389–398.

Barlow, D. J., and J. M. Thornton. 1988. Helix geometry in proteins. *J. Mol. Biol.* 201:601–619.

Barranger-Mathys, M., and D. S. Cafiso. 1996. Membrane structure of voltage-gated channel-forming peptides revealed by site-directed spin labeling. *Biochemistry.* 35:498–505.

Bechinger, B. 1997. Structure and functions of channel-forming peptides: magainins, cecropins, mellitin and alamethicin. *J. Membr. Biol.* 156: 197–211.

Brandl, C. J., and C. M. Deber. 1986. Hypothesis about the function of membrane-buried proline residues in transport proteins. *Proc. Natl. Acad. Sci. USA.* 83:917–921.

Coronado, R., and R. Latorre. 1983. Formation of phospholipid bilayers from monolayers in patch-clamp pipettes. *Biophys. J.* 43:231–236.

D'Aquino, J. D., J. Gomez, V. J. Hilser, K. H. Lee, L. M. Amzel, and E. Freire. 1996. The magnitude of the backbone conformational entropy change in protein folding. *Proteins.* 25:143–156.

Dathe, M., C. Kaduk, E. Tachikawa, M. F. Melzig, H. Wenschuh, and M. Bienert. 1998. Proline at position 14 of alamethicin is essential for hemolytic activity, catecholamine secretion from chromaffin cells and enhanced metabolic activity in endothelial cells. *Biochim. Biophys. Acta.* 1370:175–183.

Duclohier, H., G. Molle, J.-Y. Dugast, and G. Spach. 1992. Prolines are not essential residues in the "barrel-stave" model for ion channels induced by alamethicin analogs. *Biophys. J.* 63:868–873.

Esposito, G. J. A., J. A. Carver, J. Boyd, and I. D. Campbell. 1987. High-resolution 1H NMR study of the solution structure of alamethicin. *Biochemistry.* 26:1043–1050.

Fischer, G. 1995. Peptidyl-prolyl cis/trans isomerases and their effects. *Angew. Chem., Int. Ed. Engl.* 33:1415–1436.

Fox, R. O., and F. M. Richards. 1982. A voltage-gated ion channel inferred from the crystal structure of alamethicin at 1.5 Å resolution. *Nature.* 300:325–330.

Franklin, C. J., J. F. Ellena, S. Jayasinghe, L. P. Kelsh, and D. S. Cafiso. 1994. The structure of micelle-associated alamethicin from 1H NMR. Evidence for conformational heterogeneity in a voltage-gated peptide. *Biochemistry.* 33:4036–4045.

Gibbs, N., R. B. Sessions, P. B. Williams, and C. E. Dempsey. 1997. Helix bending in alamethicin: molecular dynamics simulations and amide hydrogen exchange in methanol. *Biophys. J.* 72:2490–2495.

Grathwohl, C., and K. Wuthrich. 1981. NMR studies of the rates of proline cis-trans isomerization in oligopeptides. *Biopolymers.* 20:2623–2633.

Hall, J. E., I. Vodyanoy, T. M. Balasubramanian, and G. R. Marshall. 1984. Alamethicin: a rich model for channel behavior. *Biophys. J.* 45:233–247.

Hanke, W., C. Methfessel, H. U. Wilmsen, and G. Boheim. 1984. Ion channel reconstitution into planar lipid bilayers on glass pipettes. *Bioelectrochemistry and Bioenergetics.* 12:329–339.

Helluin, O., S. Bendahhou, and H. Duclohier. 1998. Voltage sensitivity and conformational changes of isolated voltage sensors of sodium channels are tuned to proline. *Eur. Biophys. J.* 27:595–604.

Kaduk, C., H. Duclohier, M. Dathe, H. Wenschuh, M. Beyermann, G. Molle, and M. Bienert. 1997. Influence of proline position upon the ion channel activity of alamethicin. *Biophys. J.* 72:2151–2159.

Keith, A., G. Bulfield, and W. Snipes. 1970. Spin-labeled Neurospora mitochondria. *Biophys. J.* 10:618–629.

Kelsh, L. P., J. F. Ellena, and D. S. Cafiso. 1992. Determination of the molecular dynamics of alamethicin using 13C NMR: implications for the mechanism of gating of a voltage-dependent channel. *Biochemistry.* 31:5136–5144.

Krugh, T. R. 1976. Spin-label-induced nuclear magnetic resonance relaxation studies of enzymes. *In* Spin Labeling, Theory and Applications. Academic Press, New York. 339–372.

Li, S.-C., N. K. Goto, K. A. Williams, and C. M. Deber. 1996. α-Helical, but not β-sheet, propensity of proline is determined by peptide environment. *Proc. Natl. Acad. Sci. USA.* 93:6676–6681.

McConnell, H. M. 1967. Comment on article by Sternlicht and Wheeler. *In* Magnetic Resonance in Biological Systems. Pergamon, Oxford. 335.

Montal, M., and P. Mueller. 1972. Formation of bimolecular membranes form monolayers and study of their properties. *PNAS.* 69:3561–3566.

Nordio, P. L. 1976. General magnetic resonance theory. *In* Spin Labeling, Theory and Applications. Academic Press, New York. 5–52.

North, C. L., C. J. Franklin, R. G. Bryant, and D. S. Cafiso. 1994. Molecular flexibility demonstrated by paramagnetic enhancements of nuclear relaxation. Application to alamethicin: a voltage-gated peptide channel. *Biophys. J.* 67:1861–1866.

Reimer, U., N. E. Mokdad, M. Schutkowski, and G. Fischer. 1997. Intramolecular assistance of cis/trans Isomerization of the histidine-proline moiety. *Biochemistry.* 36:13802–13808.

Richardson, J. S., and D. C. Richardson. 1988. Amino acid preferences for specific locations at the ends of alpha helices. *Science.* 240:1648–1652.

Richardson, J. S., and D. C. Richardson. 1989. Prediction of Protein Structure and the Principles of Protein Conformation. Plenum Press, New York. 1–99.

Sankararamakrishnan, R., and S. Vishveshwara. 1990. Conformational studies on peptides with proline in the right-handed alpha-helical region. *Biopolymers.* 30:287–298.

Sansom, M. S. P. 1992. Proline residues in transmembrane helices of channel and transport proteins: a molecular modelling study. *Protein Eng.* 5:53–60.

Sessions, R. B., N. Gibbs, and C. E. Dempsey. 1998. Hydrogen bonding in helical polypeptides from molecular dynamics simulations and amide hydrogen exchange analysis: alamethicin and melittin in methanol. *Biophys. J.* 74:138–152.

Sternlicht, H., and E. Wheeler. 1967. Preliminary magnetic resonance studies of spin labeled macromolecules. *In* Magnetic Resonance in Biological Systems. Pergamon, Oxford. 325–334.

Stewart, J. M., and J. D. Young. 1984. Solid Phase Peptide Synthesis. Pierce Chemical Co., Rockford, IL.

Vogel, H., L. Nilsson, R. Rigler, S. Meder, G. Boheim, W. Beck, H.-H. Kurth, and G. Jung. 1993. Structural fluctuations between two conformational states of a transmembrane helical peptide are related to its channel-forming properties in planar lipid membranes. *Eur. J. Biochem.* 212:305–313.

Wenschuh, H., M. Beyermann, H. Haber, J. K. Seydel, E. Krause, M. Mienert, L. A. Carpino, A. El-Faham, and F. Albericio. 1995. Stepwise automated solid phase synthesis of naturally occurring peptaibols using FMOC amino acid fluorides. *J. Org. Chem.* 60:405–410.

Williams, K. A., and C. M. Deber. 1991. Proline residues in transmembrane helices: structural or dynamic role? *Biochemistry.* 30:8919–8923.

Woolfson, D. N., and D. H. Williams. 1990. The influence of proline residues on alpha-helical structure. *FEBS Lett.* 277:185–188.

Wuthrich, K. 1986. NMR of Proteins and Nucleic Acids. John Wiley and Sons, New York. 162–166.